miR-491-5p inhibits Emilin 1 to promote fibroblasts proliferation and fibrosis in gluteal muscle contracture via TGF-β1/Smad2 pathway

Shuai Chen[1,2*#], Qiuwan Wu[3#], Yang Wang[4], Jie Xu[5], Ye Wang[1,2], Xianyang Luo[1,2*]

Short title: Role of miR-491-5p/Emilin1 in gluteal muscle contracture.

[1]Department of Otolaryngology-Head and Neck Surgery, The First Affiliated Hospital of Xiamen University, Xiamen, Fujian 361005, P.R. China

[2]Xiamen Key Laboratory of Otolaryngology Head and Neck Surgery, Xiamen, Fujian 361005, P.R. China

[3]Department Science and Technology, The First Affiliated Hospital of Xiamen University, Xiamen, Fujian 361005, P.R. China.

[4]Sports Department of Tianjin Cheng Jian University, Tianjin 300384, China

[5]Department of Science and Technology, Tianjin University of Sport, Tianjin 300381, China

[#]These authors contributed equally to this study.

***Correspondence to:** Shuai Chen or Xianyang Luo Department of Otolaryngology-Head and Neck Surgery, The First Affiliated Hospital of Xiamen University, No. 55 Zhenhai Rd., Siming District, Xiamen 361005, Xiamen, China. Tel.: +86 18030176277; E-mails: chenshuai@xmu.edu.cn or lxy701@126.com.

Summary

Gluteal muscle contracture (GMC) is a chronic fibrotic disease of gluteal muscles due to multiple etiologies. Emilin 1 plays a determinant role in fibers formation, but its role in the progression of GMC remains unclear. The present study was aimed to search for the predictive role and regulatory mechanism of Emilin 1 on GMC. Here, Protein and mRNA expression of Emilin 1 were decreased in GMC tissues compared to normal muscle tissues. Using the anslysis of target prediction, Emilin 1 was observed to be a potential downstream sponge of miR-491-5p. In comparison to Emilin 1, miR-491-5p showed a aberrant elevation in GMC tissues, which was further proven to have a negative correlation with Emilin 1. The direct binding of miR-491-5p to Emilin 1 mRNA was confirmed by luciferase reporter gene assay, and miR-491-5p mimics inhibited, while miR-491-5p inhibitor promoted the protein expression and secretion of Emilin 1 in contraction bands (CB) fibroblasts. Additionally, miR-491-5p mimics promoted the expression of cyclin-dependent kinase 2 and cyclin D1 and the proliferation of CB fibroblasts, which could be reversed by Emilin 1 overexpression. Mechanistically, miR-491-5p mimics possibly activated transforming growth factor β1 (TGF-β1)/Smad3 signal cascade via binding to 3'-untranslated region of *Emilin 1* mRNA, thereby promoting the progression of fibrosis of CB fibroblasts. Collectively, miR-491-5p inhibited Emilin 1 expression, and subsequently promoted CB fibroblasts proliferation and fibrosis via activating TGF-β1/Smad3 signal axis. MiR-491-5p might be a potentially effective biomarker for predicting GMC, providing a novel therapeutic strategy for GMC.

Keywords: Gluteal muscle contracture; MiR-491-5p; Emilin 1; fibroblasts

Introduction

Gluteal muscle contracture (GMC) is a kind of fibrotic disease, featured by degeneration and contracture of gluteal muscle fibers and fascia [1]. GMC is first reported in 1970, and there appear numerous cases in recent decades wordwide. Various causes and pathogenesis have been hypothesized, the most common reason is supposed to be repeated intramuscular injections into the buttocks [2]. GMC is diagnosed mainly through clinical features and radiology such as computed tomography (CT), magnetic resonance imaging (MRI) and ultrasound (USG) [3]. For the treatment of GMC, there are four commonly used options including non-operative treatment, different operative treatments, programmed rehabilitation and physiotherapy, and the the preferred strategy for advanced GMC patients is surgical operation even though its effect is poor [3-4]. Therefore, it is urgent to screen novel predicting biomarkers to contribute to the diagnosis, treatment and drug development of GMC.

Elastin microfibril interfacer 1 (*Emilin 1*) is characterized by the N-terminal microfibril interface domain, the coiled α-helix domain, the collagen domain and the C-terminal spherical C1q domain and is responsible for encoding the extracellular matrix glycoprotein [5]. Emilin 1 is related to elastic fibers formation at the interface between elastin and microfibers, and may play a role in the formation of elastic tissues, including large blood vessels, dermis, heart, and lung organs [6]. Emilin 1 deletion leads to formation of elastic fibers which is related to contracture progression [7-8]. It is reported that, compared with the textured tissues, the smoother tissues are proven to produce more contractures which is attributed to more fibrils of elastin and myofibroblasts found in the smooth tissues [8]. In aortic valve disease, Emilin 1 deficiency leads to early valve interstitial cell activation and proliferation, and leads to late myofibroblast-like cell activation and fibrosis [9]. Thus, Emilin 1 reduction might contribute to muscle fibrosis and contracture formation, both of them are the major characteristics of GMC. However, whether Emilin 1 involves an ability to regulate the formation of GMC needs to be further clarified.

Transforming growth factor-beta (TGF-β) has been reported to independently serve as an effective tissue fibrosis factor by stimulating several signal cascades [10-11]. The

most typical signal axis mediated by TGF-β is based on Smad-2/3, which actvation is proven to function in pro-fibrotic progression [12]. In dupuytren contracture, TGF-β acts as a stimulator for extracellular matrix deposition and fibroblast proliferation [13]. Of note, TGF-β1, TGF-β3 and collagens are elevated in the development of GMC [14], and TGF-β1/Smad2 signal axis is confirmed to have a stimulating effect on GMC disease [15]. Furthermore, Emilin 1 has been reported to inhibit TGF-β signaling via specifically binding to the proTGF-β precursor [16]. Some studies demonstrate that Emilin 1-depleted null mice appear activated vascular TGF-β signaling and suffer from hypertension [17]. Possibly, Emilin 1 also participates in the formation of GMC via TGF-β/Smad2/3 signaling cascades.

miRNAs are key players in fibrotic disease [18-19]. Integrated miRNA expression analysis provides several potential dysregulated miRNAs in liver fibrosis [20]. In muscle-related diseases, miR-133b depletion inhibits muscle fibre regeneration, satellite cell proliferation and differentiation in pathogenesis of duchenne muscular dystrophy [21]. MiR-378 deletion attenuates muscular dystrophy in MDX mice [22]. Noticeably, several miRNAs have been proposed as the effective diagnostic biomarkers for GMC. MiR-29a exerts protective effect against fibrogenesis in GMC [23]. Therefore, muscle miRNAs are a potentially useful and reliable biomarkers for early diagnosis of muscle fibrosis-related diseases. The screening of some potent candidate miRNAs can facilitate the diagnosis and treatment of GMC.

Herein, the expression pattern of Emilin 1 and miR-491-5p and their association in GMC tissues were observed. Emilin 1 was possibly the downstream sponge of miR-491-5p, thereby taking part in the proliferation and fibrosis progresses in contraction bands (CB) fibroblasts. Our results contributed to the discovery of potential biomarkers and therapeutic target for GMC.

MATERIALS AND METHODS

Clinical specimens

This study was approved by the ethics committee of the First Affiliated Hospital of Xiamen University. All patients had signed informed consent. Human fresh contraction

bands (CB) tissues were collected from GMC patients (n=15) who received CB releasing surgery according to previous study [23]. The clinical features of the cohort were presented in **Table 1**. Gluteal muscle contracture tissues and matched adjacent normal muscle tissues were gifted from Guangdong General Hospital and Peking University Shenzhen Hospital. Briefly, part of CB tissue samples were embedded by paraffin for immuohistochemistry. The rest of CB tissues were used to perform protein and total mRNA extraction.

Immunohistochemistry (IHC)

Tissue sections were deparaffinized and immersed in xylene for 20 minutes, followed by the dehydration with a gradient of absolute ethanol. After three times washing with phosphate buffered solution-Tween 20 (PBST), 3% H_2O_2 was used to incubate with the sections for 5-10 minutes to remove endogenous peroxidase. Then, the slices were rinsed with PBS for 2-5 min and subsequently blocked with 5% BSA for 1 h. Then, the slices were incubated with primary antibody against Emilin 1 (1:200, ab243324, Abcam) at 4 ℃ overnight. The slices were washed three times with PBS, followed by incubation with horseradish peroxidase (HRP)-conjugated secondary antibody (1:5,000, BOSTER Biological Technology, BA1054). DAB chromogenic agent was added for 20 second and then the slices were counterstained with hematoxylin. In the end, the slices were dehydrated, transparentized, and sealed, and the photos were captured by the microscope (OLYMPUS, BX53)

Cell isolation and culture

Fresh CB tissues were used for human CB fibroblasts isolation. Cells were isolated as previously described and cultured in Dulbecco's modified Eagle's medium (DMEM) complemented with 10% Fetal Bovin Serum, 10 μg/ml gentamicin (15750078, Invitrogen, USA), and 10 mg/ml amphotericin B (R01510, Invitrogen, USA). Medium was changed every two days. When the confluence of cells was up to 80%-90%, cells were transfected with miR-491-5p mimics/inhibitors or plasmids and the transfected cells were collected for further experiments.

ELISA

Emilin 1 levels in CB tissues, and TGF-β1, TGF-β3 and CTGF levels in CB fibroblasts were determined by ELISA according to manufacture's instruction. In brief, the supernatants of lytic CB tissues or fibroblasts were used to monitor the concentration of fibrogenic cytokines using Emilin 1 (HZ-2997, Shanghai, CN), TGF-β1 kits (88-8350-22, Invitrogen, US), TGF-β3 kits (KA4402, Abnova, US) and CTGF kits (ABIN6730903, Abnova, US). Finally, the optical density (OD value) was measured with a microplate reader (Thermo, MULTISKAN MK3) at the wavelength of 450 nm.

RNA extraction and quantitative real-time PCR

Total RNA was extracted from CB tissues or fibroblasts with Trizol reagent (15596-026, Ambion) and the miRNeasy Mini Kit (Qiagen, Germany), respectively. For cDNA synthesis, 1,000 ng RNA in 20 μl reaction volume were used to perform reverse transcription using a HiScript Reverse Transcriptase kit (R101-01/02, VAZYME). QRT PCR was performed utilizing SYBR Green Master Mix (Q111-02, VAZYME) by a Real-Time PCR Detection System (ABI, Quant Studio 6). Stem-loop-specific primer method was applied to measure expression levels of miR-491-5p. Primer sequences were showed as **Table 2**. *Gapdh* and *U6* were used as internal reference gene. Relative gene levels were calculated using the $2^{-\Delta\Delta Ct}$ method.

Western blot

Total protein was extracted using RIPA lysis buffer. For CB tissues, tissue homogenates were collected and lysed with RIPA lysis buffer. For cultured fibroblasts, total protein was obtained using whole cell lysis after sonicating for 15 s. Bicinchoninic acid assay (BCA) assay was applied to determine the protein concentration. 20 μg protein were separated in a 10% sodium dodecyl sulfate-polyacrylamide gel electrophoresis (SDS-PAGE) and transferred onto polyvinylidene fluoride membranes (IPVH00010, Millipore, Billerica, MA, US). After blocking with 5% no-fat milk that diluted in 0.1% TBST for 1.5 h at room temperature, bands were incubated with primary antibodies against Emilin 1 (1:1000, ab243324, Abcam), CDK2 (1:1000, 18048S, Cell Signalling Technology), Cyclin D1 (1:1000, 55506S, Cell Signalling Technology), p-Smad2 (1:1000, 18338S, Cell Signalling Technology), Smad2 (1:1000, 5339S, Cell Signalling

Technology), and TGF-β1 (1:1000, 3709S, Cell Signalling Technology) at 4 °C overnight. Subsequently, bands were washed three times with TBST and incubated with HRP-conjugated secondary antibodies (1:5,000 in TBST) for 1 h at room temperature. Finally, immunoblots were then incubated with ECL chemiluminescence reagent kit and visualized with ChemiDoc XRS+System (Bio-Rad, Hercules, CA, USA). Image j software was applied to determine the intensity of each band.

Plasmids construction and transfection

Coding sequence (CDS) frangents of *Emilin 1* gene was amplified using cDNA extracted from HEK-293T cells and then sub-cloned into virus pBOBi vector. For lenti-virus packaging, HEK293T cells were firstly seeded in culture plates and co-transfected with lenti-viral vectors and packaging vectors including pMDL, VSVG, and REV at a ratio of 10:5:3:2 using polyethylenimine linear (PEI, 40816ES03, Yeasen, Shanghai, CN). After 48 h of transfection, medium were collected, concentrated and then added to CB fibroblasts in the presence of 10 μg/mL polybrene (Sigma, H9268) with fresh complete DMEM medium at a ratio of 1:1. Medium was replaced after 24 h. MiR-491-5p mimics and inhibitors were synthesized by RiboBIO Co., LTD (Guangzhou, CN) and subsequently transfected into fibroblasts with Lipofectamine^{TM} 2000 (Invitrogen,11668-019) for 48 h when the confluence reached more than 80%.

Dual-luciferase assay

Untranslated regions sequence (3'-UTR) of Emilin containing miR-491-5p binding domain and its mutant sequence were synthesized by RiboBIO Co., LTD and inserted into the pYr-MirTarget basic vector. Plasmids were co-transfection into CB fibroblasts with the Lipofectamine 2000 transfection reagent (Invitrogen, 11668-019). After treated with 48 h, cells were lysed in a reporter lysis buffer (Promega, E1910, US). The firefly luciferase activities were measured with the Dual-Glo Luciferase Assay System (Promega) in a single channel luminometer. The relative luciferase activity was calculated as the ratio of firefly luciferase activity to renilla luciferase activity.

CCK8 assay

Cell Counting Kit-8 (CCK8, MCE, HY-K0301, US) was employed to determine cell viability. In brief, primary human CB fibroblasts were inoculated into 96-well plates

(1×10^3 cells per well) for indicated time points (24h, 48h and 96h). Subsequently, 10 μL CCK-8 solution was added to each well followed by 2 h incubation. Finally, the absorbance of each sample was measured at a wavelength of 450 nm using a microplate reader (Thermo, MULTISKAN MK3).

Statistic analysis

All experiments were performed thrice at least. All data were presented as means ± SD. Differences between groups were tested using Student's t-test or one-way ANOVA followed by Tukey's post hoc tests by Graph Pad Prism software (version 9.0). Correlation analysis was performed by Pearson's coefficient using SPSS software (version 25.0). P value < 0.05 was considered as significant differences.

RESULTS

Emilin 1 is apparently reduced in GMC patients

Firstly, we evaluated the expression of Emilin 1 in GMC tissues and the paired normal muscles. As shown in figure 1A, Emilin 1 was observed to be downregulated in GMC tissues (n=15) compared to that in the corresponding normal muscle tissues by using ELISA assay (**Figure 1A**). Consistently, the mRNA level of *Emilin 1* in GMC tissues was also lower than that in normal adhesive muscle tissues (**Figure 1B**). Besides, IHC results further confirmed that Emilin 1 expression reduced significantly in GMC tissues compared to that of normal muscle tissues (**Figure 1C**). Simultaneously, the protein expression of Emilin 1 in GMC tissues (n=8) was declined robustly compared with control muscle samples (n=7) (P < 0.05, **Figure 1D**). All these findings indicated that Emilin 1 was at a low level in GMC tissues and might be a prognostic maker for GMC.

Emilin 1 are negatively correlated with miR-491-5p

Based on the online-prediction tools, such as ENCORI, TargetScan and miRWalk, miR-491-5p was identified as a potential candidate binding partner of *Emilin 1* gene (**Figure 2A**). Additionally, miR-491-5p was apparently elevated in GMC tissues compared with normal muscle tissues, which showed a totally reversed tendency with Emilin 1 (**Figure 2B**). Furthermore, correlation analysis showed that Emilin 1 and miR-

491-5p were negatively correlated in GMC tissues (**Figure 2C**). Possibly, the decreased Emilin 1 in GMC samples was related to the elevation of miR-491-5p.

miR-491-5p sponges Emilin 1 in fibroblasts

Although miR-491-5p was predicted to bind to Emilin 1 mRNA (**Figure 3A**, the upper sequence), whether miR-491-5p could regulate the transcriptional activity of Emilin 1 remained vague. In reporter gene assay, miR-491-5p mimics transfection significantly reduced the transcriptional activity of Emilin 1 in cells transfected with Emilin 1-WT reporter plasmid, but had no impact on its luciferase activity in cells transfected with Emilin 1-Mut reporter plasmid (**Figure 3A**). Besides, miR-491-5p could negatively regulated Emilin 1 protein expression in primary fibroblasts isolated from contracture tissues, showing a decrease in miR-491-5p mimics-transfected cells and an increase in miR-491-5p inhibitor-transfected cells (**Figure 3B**). Equally, Emilin 1 secreted from fibroblasts was also negatively regulated by miR-491-5p (**Figure 3C**). The effects of miR-491-5p mimics and miR-491-5p inhibitor were confirmed using qRT-PCR assay (**Figure S1**). Thus, miR-491-5p negatively regulated the transcription of *Emilin 1* via directly binding to 3'-untranslated region (3'-UTR) of *Emilin 1* gene.

miRNA/Emilin 1 signal axis regulates proliferation of fibroblasts

Next, the role of miRNA/Emilin 1 pathway on cell proliferation was explored in fibroblasts. Once cells were administrated with miR-491-5p mimics, cell viability notably accelerated on day 3 and day 4, whereas miR-491-5p inhibitors transfection could remarkably slow down the growth capability compared to control cells transfected with negative inhibitor (**Figure 4A**). Thus, miR-491-5p positively affected cell growth of fibroblasts. Subsequently, the biological function of Emilin 1 in miR-491-5p-transfected fibroblasts was also evaluated. As shown in figure 4B, overexpression of Emilin 1 reversed the proliferation promotion effects induced by miR-491-5p mimics (**Figure 4B**). As expected, miR-491-5p mimics apparently elevated the protein expression of cell cycle-related molecules including CDK2 and Cyclin D1, which were restored by the transfection of exogenous Emilin 1 (**Figure**

4C&D). These results indicated that miR-491-5p promoted the proliferation of fibroblasts possibly through sponging Emilin 1.

miRNA/Emilin 1 regulates fibrotic process possibly via TGF-β/Smad2 signaling

The activation of TGF-β/Smad2 signaling was determined to further explore Emilin 1-launched signaling cascades in process of fibrotic formation. As shown in figure 5A, miR-491-5p upregulation significantly reduced Emilin 1 expression, but promoted the expression of TGF-β1 and phosphorylation of Smad2, which were notably rescued by the transfection of exogenous Emilin 1 (**Figure 5A&B**). Next, the mRNA expression of downstream fibrogenic cytokines were measured by qRT-PCR. Along with the activation of TGF-β1/Smad2 signal pathway, the contents of *Collagen I*, *Collagen III*, *α-SMA* and *Elastin* also elevated in miR-491-5p mimics-exposed cells (**Figure 5C**). Once Emilin 1 was overexpressed in miR-491-5p mimics-exposed cells, the upregulation of these fibrosis factors was notably abolished (**Figure 5C**). In addition to that, miR-491-5p mimics drastically promoted the secretion of TGF-β1, TGF-β3 and connective tissue growth factor (CTGF), which were reversed by the administration of exogenous Emilin 1 (**Figure 5D-F**). Therefore, Emilin 1 negatively regulated the expression of fibrotic cytokines through TGF-β1/Smad3 axis, resulting in the remission of fibrosis in fibroblasts.

DISCUSSION

GMC is a common fibrotic disease with no preonunced diagnostic biomarker and effective treatment strategies [3]. Fibroblasts and myofibroblasts significantly proliferates in GMC tissue, which is thought to be the main cause for GMC formation [24]. Herein, our research revealed that Emilin 1 cooperated with miR-491-5p to participate in the progress of GMC via regulating TGF-β1/Smad2 pathway, implying that miR-491-5p and Emilin 1 might be the promising therapy target for GMC diagnose.

The Emilin protein family are involved in maintaining the stable state of the body's tissues and organs [25]. Emilin 1 has been considered to participate in the development of elastic tissues. Loss of the cytoskeletal protein Emilin 1 induces the formation of

elastic fragments [7, 26]. In our study, there is an obvious reduction of Emilin 1 expression in GMC tissues compared with control normal muscle tissues. The declined Emilin 1 can induce the aggregation of elastic fibers, and amounts of elastic fibers can serve as prognosis of idiopathic pulmonary fibrosis [27]. The accumulation of elastic fibers can enhance the stiffness of fibrotic tissues and subsequently broken the connective tissue, leading to contracture formation [28]. Taken together, Emilin 1 might serve as a anti-fibrosis factor in muscle-related diseases via affecting elastic fibers accumulation.

MiRNAs are supposed to mediate the occurrence of muscle fibrosis disease [29]. Numerous miRNAs including miR-150, miR-194 and miR-221 are promising biomarkers in liver fibrosis [30-31]. Moreover, miRNAs-based therapeutic strategy has been applied to treat cystic fibrosis combined with nanotechnology, which further prove the potential therapeutic capability of miRNAs in fibrosis disease [32]. Of note, MiR-491 upregulation inhibits myocyte differentiation and adult muscle regeneration, indicating that miR-491 may have a negative regulatory effect on myogenic differentiation [33]. Enhanced myogenic differentiation is accompanied with a reduced degree of myogenic contracture in a rabbit model of extending knee joint contracture [34]. Thus, miR-491 potentially participates in the progression of contracture of GMC disease. However, modification effects on fibrotic events mediated by miRNAs heavily depended on miRNA-induced silencing complex that binds to downstream target messenger RNA (mRNA). Emilin 1 ihas been considered as a suitable sponge gene for miRNAs [35]. In this study, Emilin 1 was identified as a potential binding target of miR-491-5p. MiR-491-5p directly bound to *Emilin 1* mRNA, negatively regulating the expression of Emilin 1 in primary CB fibroblasts. It is proved that miR-491-5p participates in the progression of renal fibrosis [36]. All these results indicated that miR-491-5p may implicate in the progression of GMC through cooperating with Emilin 1.

Fibroblasts are main components of connective tissue in human body. Fibroblasts are reported to serve pivotal roles on pathological stage of tissue fibrosis [37]. In progressive renal disease, the interstitium is filled with fibroblasts which is much more than normal tissues [38]. It is confirmed that the enhancement of fibroblasts

proliferation and migration promote joint fibrosis [39]. Fibroblasts proliferation is elevated in fibrotic disease and GMC [15]. In our results, miR-491-5p was elevated in GMC tissues compared to control tissues. And miR-491-5p could significantly promoted the proliferation of fibroblasts. Possibly, fibroblasts proliferation mediated by miR-491-5p elevation contributed to fibrosis formation in GMC tissues. Emilin 1 deficiency can lead to fibrosis activation accompanied with fibroblasts proliferation in aortic valve disease [9]. Emilin 1 depletion accelerates elastic fibers formation thus promoting contracture progression [7]. Our result further proved that Emilin 1 overexpression abolished miR-491-5p mimics-mediated fibroblasts proliferation. Collectively, the reduced Emilin 1 mediated by endogenous miR-491-5p possibly promoted fibroblasts proliferation, followed by the formation of elastic tissue pieces, which might be one of the causes for GMC development.

Numerous fibrotic regulators such as collagens and transforming growth factor (TGF) members are reported to involve in formation of GMC [14]. MiR-29b regulates endometrial fibrosis through the blockade of the specificity protein 1 (Sp1)-TGF-β1/Smad-CTGF pathway [40]. Up-regulation of miR-491-5p contributes to TGF-β-regulated partitioning-defective protein 3 (Par-3) expression in rat proximal tubular epithelial cells [41]. Besides, miR-491 is identified as a negative regulator of skeletal muscle differentiation through targeting myomaker, which suggests that TGF-β participates in muscle-related disease [33]. Actually, miR-491 is dysregulated in lung fibrosis, resulting in inactivation of pro-fibrotic TGF-β/Smad3/NF-κB pathways [42]. In our results, miR-491-5p mimic activated TGF-β1/Smad2 signal axis, accompanied by the increase of Collagen I, Collagen III, a-SMA and Elastin. Inhibition of fibrosis-related genes, such as alpha-1 type I collagen (COL1A1) and alpha-1 type VI collagen (COL6A1) lead to the suppression of fibrosis progression [43]. It is reported that miR-29b-3p mimic attenuates liver fibrosis through downregulating α-SMA, COL1A1, and COL3A1 [44]. Therefore, our data further proved that miR-491-5p-mediated fibroblasts proliferation possibly involved in the fibrogenic process via activating TGF-β1/Smad2 signal pathway. Emilin1 is also necessary for elastogenesis by inhibiting TGF-β signaling [7]. Fibroblasts proliferation is demonstrated to be elevated due to the absent

of emilin1-integrin interactions in emilin1-deficient mice [45]. Herein, Emilin 1 overexpression reversed the pro-fibrostic effect of miR-491-5p in fibroblasts, indicating that miR-491-5p-mediated activation of TGF-β/Smad2 pathway and fibrostic process depended on Emilin 1 in fibroblasts. These findings firstly revealed that miR-491-5p participated in the progression of GMC through regulating Emilin 1 and the downstream TGF-β/Smad2 signal axis. However, sample size is limited in this research. Additionally, whether miR-491-5p/Emilin 1-induced fibrosis depends on fibroblasts proliferation remains to be explored in the next study.

Conclusion

In conclusion, miR-491-5p directly bind to *Emilin 1* mRNA and negatively regulated the expression of Emilin 1, and subsequently promote the proliferation and fibrotic progression in fibroblasts via activating TGF-β/Smad2 signal axis. MiR-491-5p and Emilin 1 might be served as the early diagnosis biomarkers for GMC. These results may provide potential predictive and treatment targets for GMC therapy.

Acknowledgments

This work was funded by Natural Science Foundation of Fujian Province (2020J05302, 2021J011358 and 2019J01575), Natural Science Basic Research Program of Shaanxi Province (2021JQ-780), National Natural Science Foundation of China (81802332), Xiamen Science and Technology Bureau (3502Z20209266) and Science Foundation of the Fujian provincial Commission of Health and Family Planning, China (2019-ZQNB-27 and 2021GGB026).

REFERENCES

1. Ye B, Zhou P, Xia Y, Chen Y, Yu J, Xu S. New minimally invasive option for the treatment of gluteal muscle contracture. Orthopedics 2012;35:e1692-1698. https://doi: 10.3928/01477447-20121120-11.

2. Scully WF, White KK, Song KM, Mosca VS. Injection-induced gluteus muscle contractures: diagnosis with the "reverse Ober test" and surgical management. J Pediatr Orthop 2015;35:192-198. https://doi: 10.1097/BPO.0000000000000238.

3. Rai S, Meng C, Wang X, Chaudhary N, Jin S, Yang S, Wang H. Gluteal muscle contracture: diagnosis and management options. SICOT J 2017;3:1-10. https://doi: 10.1051/sicotj/2016036.

4. Liu G, Yang S, Du J, Zheng Q, Shao Z, Yang C. Treatment of severe gluteal muscle contracture in children. J Huazhong Univ Sci Technolog Med Sci 2008;28:171-173. https://doi: 10.1007/s11596-008-0214-6.

5. Colombatti A, Spessotto P, Doliana R, Mongiat M, Bressan GM, Esposito G. The EMILIN/Multimerin family. Front Immunol 2011;2:1-13. https://doi: 10.3389/fimmu.2011.00093.

6. Bressan GM, Daga-Gordini D, Colombatti A, Castellani I, Marigo V, Volpin D. Emilin, a component of elastic fibers preferentially located at the elastin-microfibrils interface. J Cell Biol 1993;121:201-212. https://doi: 10.1083/jcb.121.1.201.

7. Zanetti M, Braghetta P, Sabatelli P, Mura I, Doliana R, Colombatti A, Volpin D, Bonaldo P, Bressan GM. EMILIN-1 deficiency induces elastogenesis and vascular cell defects. Mol Cell Biol 2004;24:638-650. https://doi: 10.1128/MCB.24.2.638-650.2004.

8. Kuriyama E, Ochiai H, Inoue Y, Sakamoto Y, Yamamoto N, Utsumi T, Kishi K, Okumoto T, Matsuura A. Characterization of the Capsule Surrounding Smooth and Textured Tissue Expanders and Correlation with Contracture. Plast Reconstr Surg Glob Open 2017;5:1-7. https://doi: 10.1097/GOX.0000000000001403.

9. Munjal C, Opoka AM, Osinska H, James JF, Bressan GM, Hinton RB. TGF-beta mediates early angiogenesis and latent fibrosis in an Emilin1-deficient mouse model of aortic valve disease. Dis Model Mech 2014;7:987-996. https://doi: 10.1242/dmm.015255.

10. Meng XM, Nikolic-Paterson DJ, Lan HY. TGF-beta: the master regulator of fibrosis. Nat Rev Nephrol 2016;12:325-338. https://doi: 10.1038/nrneph.2016.48.

11. Kim KK, Sheppard D, Chapman HA. TGF-beta1 Signaling and Tissue Fibrosis. Cold Spring Harb Perspect Biol 2018;10:1-34. https://doi: 10.1101/cshperspect.a022293.

12. Walton KL, Johnson KE, Harrison CA. Targeting TGF-beta Mediated SMAD Signaling for the Prevention of Fibrosis. Front Pharmacol 2017;8:1-11. https://doi: 10.3389/fphar.2017.00461.

13. Kloen P, Jennings CL, Gebhardt MC, Springfield DS, Mankin HJ. Transforming growth factor-beta: possible roles in Dupuytren's contracture. J Hand Surg Am 1995;20:101-108. https://doi: 10.1016/S0363-5023(05)80067-X.

14. Zhao CG, He XJ, Lu B, Li HP, Kang AJ. Increased expression of collagens, transforming growth factor-beta1, and -beta3 in gluteal muscle contracture. BMC Musculoskelet Disord 2010;11:1-8. https://doi: 10.1186/1471-2474-11-15.

15. Zhang X, Ma Y, You T, Tian X, Zhang H, Zhu Q, Zhang W. Roles of TGF-beta/Smad signaling pathway in pathogenesis and development of gluteal muscle contracture. Connect Tissue Res 2015;56:9-17. https://doi: 10.3109/03008207.2014.964400.

16. Zacchigna L, Vecchione C, Notte A, Cordenonsi M, Dupont S, Maretto S, Cifelli G, Ferrari A, Maffei A, Fabbro C, Braghetta P, Marino G, Selvetella G, Aretini A, Colonnese C, Bettarini U, Russo G, Soligo S, Adorno M, Bonaldo P, Volpin D, Piccolo S, Lembo G, Bressan GM. Emilin1 links TGF-beta maturation to blood pressure homeostasis. Cell 2006;124:929-942. https://doi: 10.1016/j.cell.2005.12.035.

17. Carnevale D, Facchinello N, Iodice D, Bizzotto D, Perrotta M, De Stefani D, Pallante F, Carnevale L, Ricciardi F, Cifelli G, Da Ros F, Casaburo M, Fardella S, Bonaldo P, Innocenzi G, Rizzuto R, Braghetta P, Lembo G, Bressan GM. Loss of EMILIN-1 Enhances Arteriolar Myogenic Tone Through TGF-beta (Transforming Growth Factor-beta)-Dependent Transactivation of EGFR (Epidermal Growth Factor Receptor) and Is Relevant for Hypertension in Mice and Humans. Arterioscler Thromb Vasc Biol 2018;38:2484-2497. https://doi: 10.1161/ATVBAHA.118.311115.

18. Jiang X, Tsitsiou E, Herrick SE, Lindsay MA. MicroRNAs and the regulation of fibrosis. FEBS J 2010;277:2015-2021. https://doi: 10.1111/j.1742-4658.2010.07632.x.

19. Fan Y, Chen H, Huang Z, Zheng H, Zhou J. Emerging role of miRNAs in renal fibrosis. RNA Biol 2020;17:1-12. https://doi: 10.1080/15476286.2019.1667215.

20. Ye M, Wang S, Sun P, Qie J. Integrated MicroRNA Expression Profile Reveals Dysregulated miR-20a-5p and miR-200a-3p in Liver Fibrosis. Biomed Res Int 2021;2021:1-10. https://doi: 10.1155/2021/9583932.

21. Taetzsch T, Shapiro D, Eldosougi R, Myers T, Settlage RE, Valdez G. The microRNA miR-133b functions to slow Duchenne muscular dystrophy pathogenesis. J Physiol 2021;599:171-192. https://doi: 10.1113/JP280405.

22. Podkalicka P, Mucha O, Bronisz-Budzynska I, Kozakowska M, Pietraszek-Gremplewicz K, Cetnarowska A, Glowniak-Kwitek U, Bukowska-Strakova K, Ciesla M, Kulecka M, Ostrowski J, Mikula M, Potulska-Chromik A, Kostera-Pruszczyk A, Jozkowicz A, Loboda A, Dulak J. Lack of miR-378 attenuates muscular dystrophy in mdx mice. JCI Insight 2020;5:1-19. https://doi: 10.1172/jci.insight.135576.

23. Zhou R, Ren S, Li C, Zhang X, Zhang W. miR-29a is a potential protective factor for fibrogenesis in gluteal muscle contracture. Physiol Res 2020;69:467-479. https://doi: 10.33549/physiolres.934295.

24. Yuan BT, Qu F, Wang SX, Qi W, Shen XZ, Li CB, Liu YJ. Histology and molecular pathology of iliotibial tract contracture in patients with gluteal muscle contracture. Biosci Rep 2019;39:1-8. https://doi: 10.1042/BSR20181351.

25. Imhof T, Korkmaz Y, Koch M, Sengle G, Schiavinato A. EMILIN proteins are novel extracellular constituents of the dentin-pulp complex. Sci Rep 2020;10:1-12. https://doi: 10.1038/s41598-020-72123-2.

26. Danussi C, Spessotto P, Petrucco A, Wassermann B, Sabatelli P, Montesi M, Doliana R, Bressan GM, Colombatti A. Emilin1 deficiency causes structural and functional defects of lymphatic vasculature. Mol Cell Biol 2008;28:4026-4039. https://doi: 10.1128/MCB.02062-07.

27. Enomoto N, Suda T, Kono M, Kaida Y, Hashimoto D, Fujisawa T, Inui N, Nakamura Y, Imokawa S, Funai K, Chida K. Amount of elastic fibers predicts prognosis of idiopathic pulmonary fibrosis. Respir Med 2013;107:1608-1616. https://doi: 10.1016/j.rmed.2013.08.008.

28. Nikolaou S, Liangjun H, Tuttle LJ, Weekley H, Christopher W, Lieber RL, Cornwall R. Contribution of denervated muscle to contractures after neonatal brachial plexus injury: not just muscle fibrosis. Muscle Nerve 2014;49:398-404. https://doi: 10.1002/mus.23927.

29. O'Reilly S. MicroRNAs in fibrosis: opportunities and challenges. Arthritis Res Ther 2016;18:1-10. https://doi: 10.1186/s13075-016-0929-x.

30. Abdel-Al A, El-Ahwany E, Zoheiry M, Hassan M, Ouf A, Abu-Taleb H, Rahim AA, El-Talkawy MD, Zada S. miRNA-221 and miRNA-222 are promising biomarkers for progression of liver fibrosis in HCV Egyptian patients. Virus Res 2018;253:135-139. https://doi: 10.1016/j.virusres.2018.06.007.

31. Venugopal SK, Jiang J, Kim TH, Li Y, Wang SS, Torok NJ, Wu J, Zern MA. Liver fibrosis causes downregulation of miRNA-150 and miRNA-194 in hepatic stellate cells, and their overexpression causes decreased stellate cell activation. Am J Physiol-Gastr L 2010;298:G101-G106. https://doi: 10.1152/ajpgi.00220.2009.

32. McKiernan PJ, Cunningham O, Greene CM, Cryan SA. Targeting miRNA-based medicines to cystic fibrosis airway epithelial cells using nanotechnology. Int J Nanomedicine 2013;8:3907-3915. https://doi: 10.2147/IJN.S47551.

33. He J, Wang F, Zhang P, Li W, Wang J, Li J, Liu H, Chen X. miR-491 inhibits skeletal muscle differentiation through targeting myomaker. Arch Biochem Biophys 2017;625-626:30-38. https://doi: 10.1016/j.abb.2017.05.020.

34. Wang F, Zhang QB, Zhou Y, Liu AY, Huang PP, Liu Y. Effect of ultrashort wave treatment on joint dysfunction and muscle atrophy in a rabbit model of extending knee joint contracture: Enhanced expression of myogenic differentiation. Knee 2020;27:795-802. https://doi: 10.1016/j.knee.2020.02.013.

35. Patel V, Noureddine L. MicroRNAs and fibrosis. Curr Opin Nephrol Hypertens 2012;21:410-416. https://doi: 10.1097/MNH.0b013e328354e559.

36. Chung AC, Lan HY. MicroRNAs in renal fibrosis. Front Physiol 2015;6:1-9. https://doi: 10.3389/fphys.2015.00050.

37. Kendall RT, Feghali-Bostwick CA. Fibroblasts in fibrosis: novel roles and mediators. Front Pharmacol 2014;5:1-13. https://doi: 10.3389/fphar.2014.00123.

38. Meran S, Steadman R. Fibroblasts and myofibroblasts in renal fibrosis. Int J Exp Pathol 2011;92:158-167. https://doi: 10.1111/j.1365-2613.2011.00764.x.

39. Xiao D, Liang T, Zhuang Z, He R, Ren J, Jiang S, Zhu L, Wang K, Shi D. Lumican promotes joint fibrosis through TGF-beta signaling. FEBS Open Bio 2020;10:2478-2488. https://doi: 10.1002/2211-5463.12974.

40. Li J, Du S, Sheng X, Liu J, Cen B, Huang F, He Y. MicroRNA-29b Inhibits Endometrial Fibrosis by Regulating the Sp1-TGF-beta1/Smad-CTGF Axis in a Rat Model. Reprod Sci 2016;23:386-394. https://doi: 10.1177/1933719115602768.

41. Zhou Q, Fan J, Ding X, Peng W, Yu X, Chen Y, Nie J. TGF-{beta}-induced MiR-491-5p expression promotes Par-3 degradation in rat proximal tubular epithelial cells. J Biol Chem 2010;285:40019-40027. https://doi: 10.1074/jbc.M110.141341.

42. Calyeca J, Balderas-Martinez YI, Olmos R, Jasso R, Maldonado V, Rivera Q, Selman M, Pardo A. Accelerated aging induced by deficiency of Zmpste24 protects old mice to develop bleomycin-induced pulmonary fibrosis. Aging (Albany NY) 2018;10:3881-3896. https://doi: 10.18632/aging.101679.

43. Heller KN, Mendell JT, Mendell JR, Rodino-Klapac LR. MicroRNA-29 overexpression by adeno-associated virus suppresses fibrosis and restores muscle function in combination with micro-dystrophin. JCI Insight 2017;2:1-13. https://doi: 10.1172/jci.insight.93309.

44. Tao R, Fan XX, Yu HJ, Ai G, Zhang HY, Kong HY, Song QQ, Huang Y, Huang JQ, Ning Q. MicroRNA-29b-3p prevents Schistosoma japonicum-induced liver fibrosis by targeting COL1A1 and COL3A1. J Cell Biochem 2018;119:3199-3209. https://doi: 10.1002/jcb.26475.

45. Danussi C, Petrucco A, Wassermann B, Pivetta E, Modica TM, Del Bel Belluz L, Colombatti A, Spessotto P. EMILIN1-alpha4/alpha9 integrin interaction inhibits dermal fibroblast and keratinocyte proliferation. J Cell Biol 2011;195:131-145. https://doi: 10.1083/jcb.201008013.

Figures and Figure legends

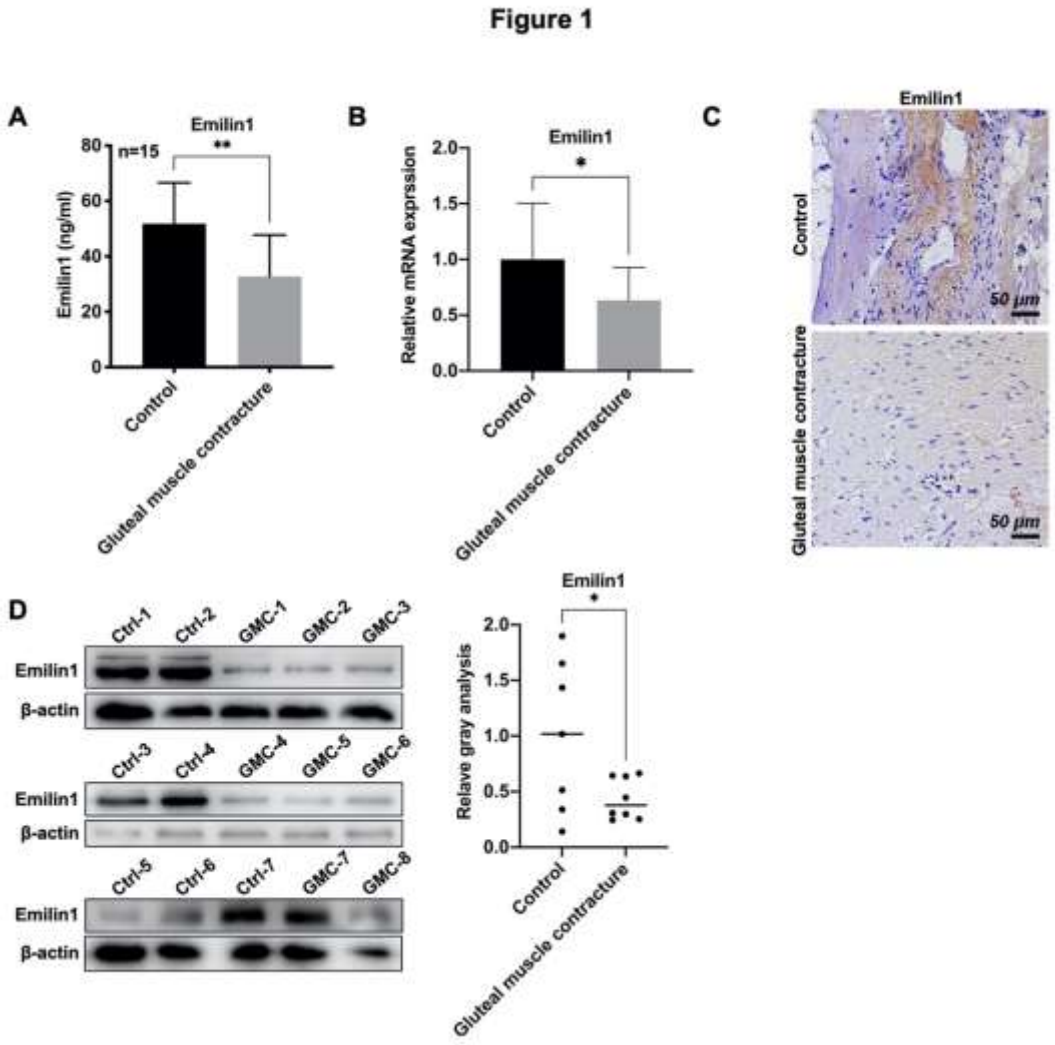

Figure 1. Expression pattern of Emilin 1 in GMC tissues. (A) ELISA assay was used to detect secretion of Emilin 1 in GMC tissues and the paired normal tissues (n=15). **(B)** qRT-qPCR assay was used to measure the expression of Emilin 1 in GMC tissues and normal tissues (n=15). **(C)** IHC staining was applied to detect the expression of Emilin 1 in GMC tissues and the paired normal tissues. **(D)** Immunoblotting with Emilin 1 antibody was conducted to determine the content of Emilin 1 in GMC group and control group (n=15). Bands density were analyzed and presented in right panel *$p<0.05$ and **$p<0.01$.

Figure 2

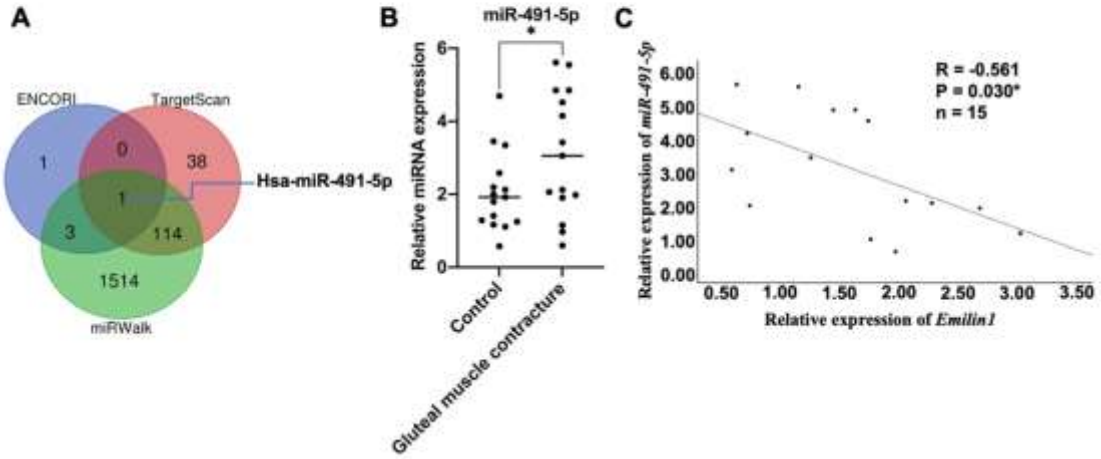

Figure 2. Association analysis between Emilin 1 and miR-491-5p. (A) Online tools were used to predict the underlying target miRNAs of Emilin 1. 153 miRNAs in TargetScan, 5 in ENCORI and 1632 in miRWALK were screened. **(B)** miR-491-5p mRNA expression in each clinical sample was determined with qRT-PCR. **(C)** The correlation between miR-491-5p and Emilin 1 was analyzed (n=15). R, pearson coefficient. Data were shown as the mean ± SD, n = 3. *p<0.05 and **p<0.01 compared with the corresponding.

Figure 3

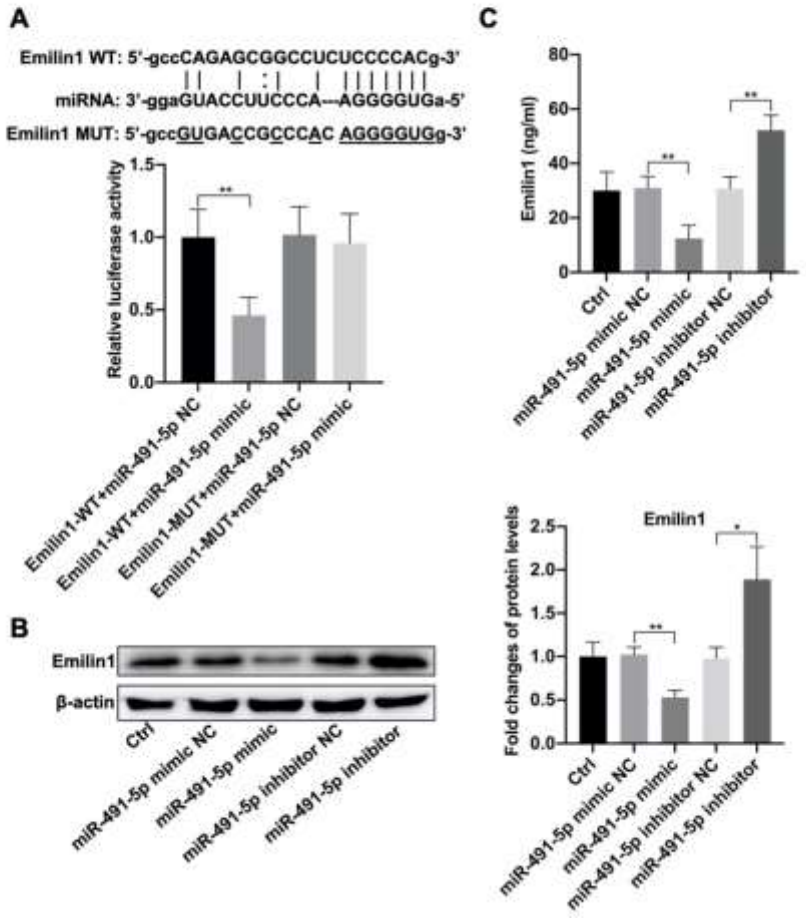

Figure 3. Regulation of miR-491-5p on Emilin 1. (A) Cells were co-transfected with wild type Emilin 1 or mutated Emilin 1 reporter plasmids, and miR-491-5p mimics or mimics control. Dual luciferase reporter gene assay was carried out to detect the binding of miR-491-5p on *Emilin 1* mRNA. **(B)** Cells were transfected with miR-491-5p mimics, inhibitors or their corresponding control mimics/inhibitor. Immunoblot assay was conducted to detect the expression of Emilin 1 in human contraction bands (CB) fibroblasts and band densities were quantified in right panel. **(C)** Cells were transfected with miR-491-5p mimics, inhibitors or their corresponding control mimics/inhibitor. Emilin 1 secretion in each group was monitored by using ELISA assay. Data were shown as the mean ± SD, n = 3. Values were significantly different compared with the corresponding control value at *$p<0.05$ and **$p<0.01$.

Figure 4

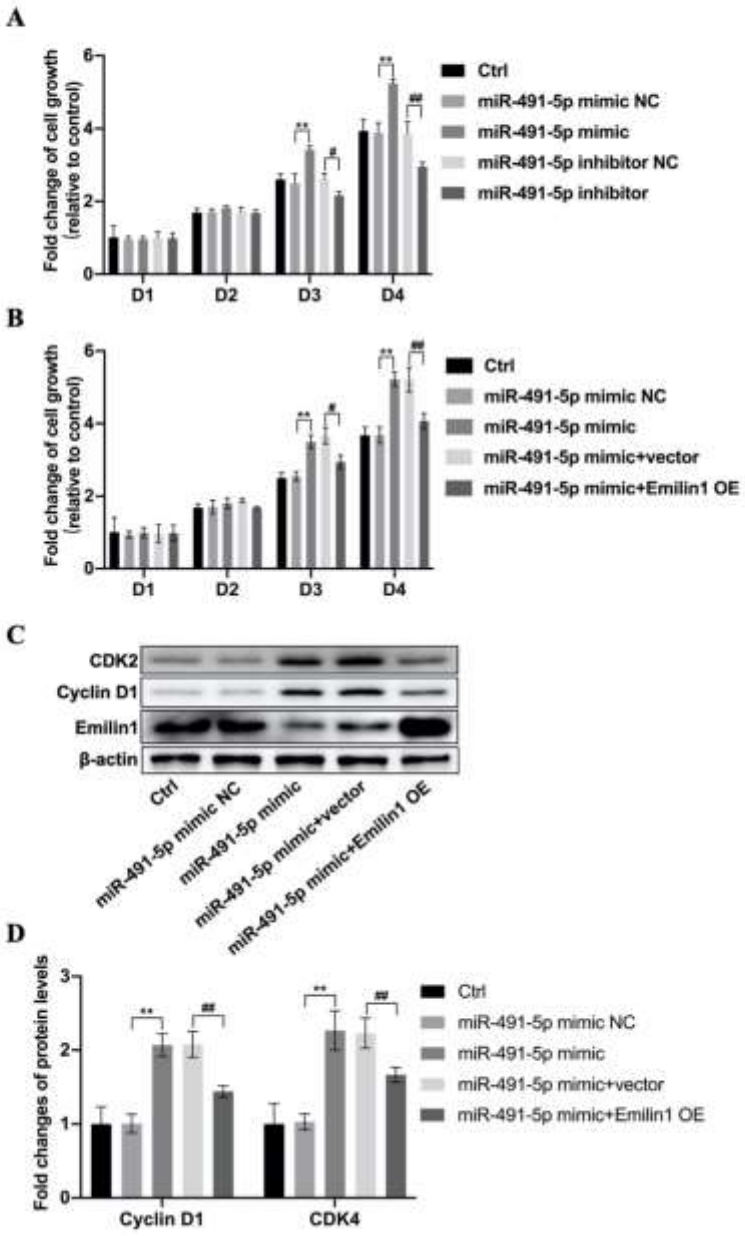

Figure 4. Effects of miR-491-5p/Emilin 1 on proliferation of CB fibroblasts. (A) Cells were transfected with miR-491-5p mimics or mimics control and inhibitors or inhibitors control. CCK8 assay was carried out to evaluate cell viability in each group. **(B)** Cells were transfected with miR-491-5p mimics or mimics control, and Emilin 1 overexpression plasmid or vector control. CCK8 assay was carried out to evaluate cell viability in each group. **(C)** Immunoblot assay was applied to measure protein expression of Cyclin D1 and CDK2. **(D)** CDK4 and Cyclin D1 expression levels were determined with grayscale. All data analysis above used One-Way ANOVA analysis of

variance. Data were shown as the mean ± SD, n = 3. *$p<0.05$ and **$p<0.01$.

Figure 5

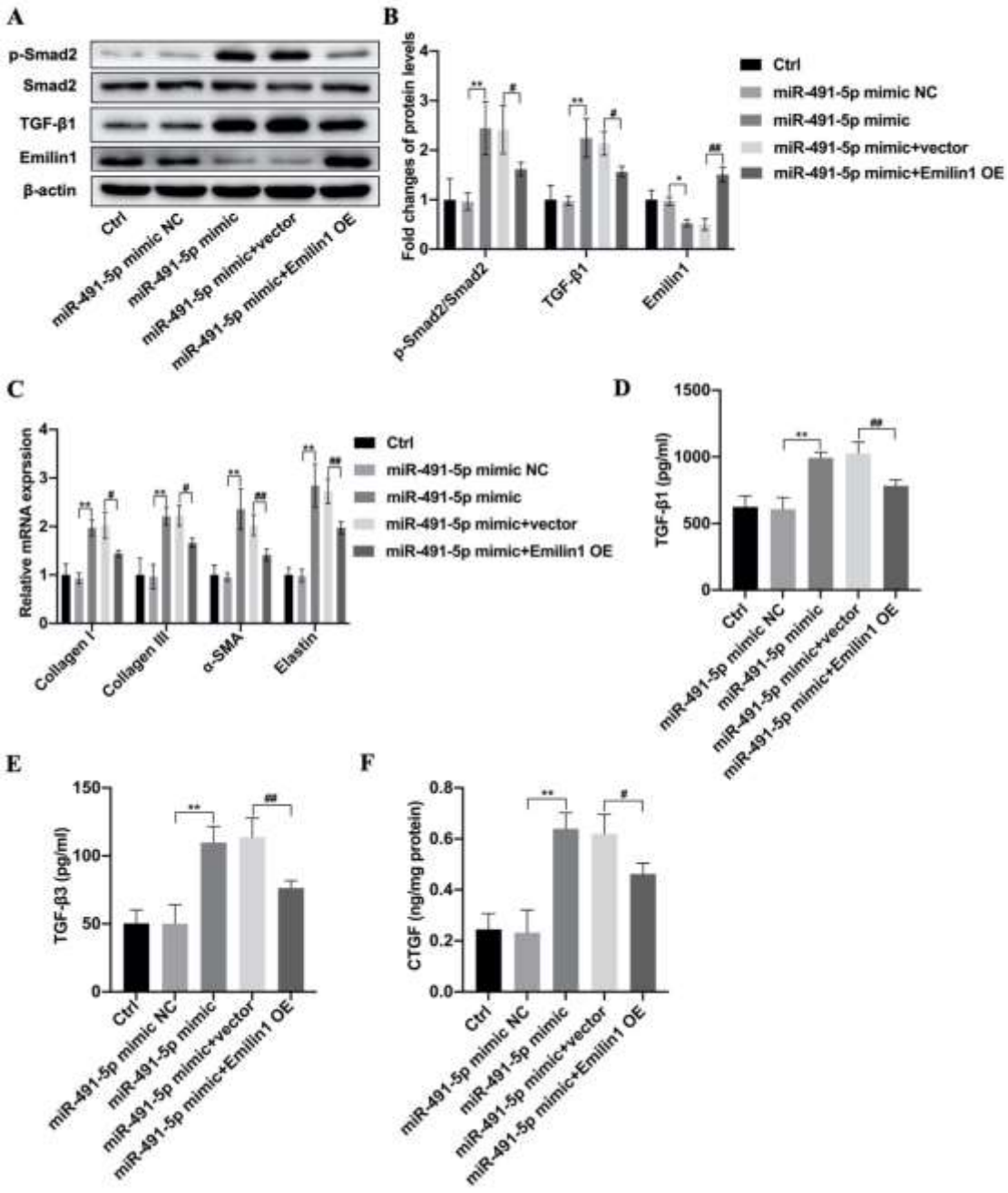

Figure 5. Role of miR-491-5p/Emilin 1 on TGF-β/Smad2 signaling axis and fibrosis. **(A)** Cells were transfected with miR-491-5p mimics or mimics control, and Emilin 1 overexpression plasmid or vector control. Western blot assay was used to evaluate the effect of miR-491-5p on TGF-β and Smad2, and β-Actin was loaded as control. **(B)** Grayscale analysis of bands in Figure A was conducted. **(C)** Cells were transfected with miR-491-5p mimics or mimics control and Emilin 1 overexpression plasmid or vector

control. mRNA levels of downstream fibrotic cytokines *Collagen I*, *Collagen III*, *a-SMA* and *Elastin* were evaluated using qRT-PCR in each group. **(D-F)** Cells were transfected with miR-491-5p mimics or mimics control and Emilin 1 overexpression plasmids or vector control. Levels of TGF-β1 **(D),** TGF-β3 **(E)** and CTGF **(F)** were evaluated with ELISA assay in each group. All data analysis above used One-Way ANOVA analysis of variance. Data were shown as the mean ± SD, n = 3. *$p<0.05$ and **$p<0.01$.

Table 1. Clinical features of GMC patients.

	Gluteal muscle contracture (GMC)
Gender	
Male	6
Female	9
Age	31.05 ± 0.974
Weight (kg)	58.24 ± 3.023
Disease type	
Bilateral GMC	15
Unilateral GMC	0
Treatment	Arthroscopic release

Table 2 Primer sequences of qRT-PCR.

Gene name	Forward (5'-3')	Reverse (5'-3')
Collagen I	GTCGAGGGCCAAGACGAAG	CAGATCACGTCATCGCACAAC
Collagen III	TGGTCCCCAAGGTGTCAAAG	GGGGGTCCTGGGTTACCATTA
αSMA	GTGTTATGTAGCTCTGGACTTTGAAAA	GGCAGCGGAAACGTTCATT
Emilin 1	ACGCTGGAGGGATTACAAGA	TCAGCCGTAGTGTGAACTCTG
Elastin	GGCCATTCCTGGTGGAGTTCC	AACTGGCTTAAGAGGTTTGCCTCCA
β-actin	CTCCATCCTGGCCTCGCTGT	GCTGTCACCTTCACCGTTCC
U6	CTTCGGCAGCACATATAC	GAACGCTTCACGAATTTGC
miR-491-5p	GGAGTGGGGAACCCTTCC	GTGCAGGGTCCGAGGT